Femtosecond Lasers Ablation: Challenges and Opportunities

L. Jiang and H. L. Tsai

Department of Mechanical and Aerospace Engineering and Engineering Mechanics, University of Missouri-Rolla, Rolla, MO 65409
Email: jianglan@umr.edu, tsai@umr.edu

Abstract

Energy transport in femtosecond laser ablation can be separated into two stages: 1) laser energy absorption by electrons during the pulse irradiation and 2) absorbed energy redistribution in bulk materials leading to material removals mostly occurring after the pulse duration. This paper reviews challenges in understanding both stages mainly for the femtosecond ablation of wide bandgap materials at the intensities on the order of 10^{13} ~ 10^{14} W/cm^2. First, major opinions and challenges in ionization mechanisms are presented by primarily considering multiphoton ionization and avalanche ionization, on the basis of experimental measurements, kinetic theory, Boltzmann equation, and molecular dynamics simulations. Next, difficulties in predicting free electron temperatures are illustrated. Then, the augments on the mechanisms of material removals are addressed with the concentration on thermal vaporization and Coulomb explosion. Finally, based on the discussions of energy transport, this paper discusses the estimation methods and unsolved problems for threshold fluence and ablation depth.

1. Introduction

Femtosecond lasers open wide-range and exciting new possibilities in microfabrications of metals [1-4], polymers [5, 6], semiconductors [7, 8], ultrahard materials [9, 10], transparent materials [11, 12], and tissues [13] for automotive industry, pharmaceutical industry, process and automation technology, defense industry, aerospace industry, information technology, telecommunication technology, biotechnology, medicine industry, measurement and microscopy, environmental technology, etc. [14-22].

A femtosecond pulse in some aspects fundamentally changes the laser-material interaction mechanism compared with a long pulse. A femtosecond laser can easily achieve very high peak power, which is powerful enough for full ionization of almost any material [23-25]. At such high intensities, seed free electrons are mainly generated by strong-electric-field ionization including multiphoton ionization and/or tunnel ionization [26], which is almost independent on the initial state of the target materials [27-29]. Hence, femtosecond laser ablation is deterministic and reproducible [30, 31]. Sub-diffraction structures can be achieved by choosing laser fluence slightly above the ablation threshold [32, 33]. Femtosecond laser-material interaction is highly nonequilibrium [34-37]. Electrons are excited up to a few to tens of electron volts (1 eV = 11,600 K for electrons) [38-40] in tens of femtoseconds [29], while the subsequent energy transfer from electrons to ions is of picosecond order [41, 42]. Hence, the ultrafast pulse energy is mainly deposited in a small layer in the photon-electron interaction process [43, 44]. Heat conduction and hydrodynamic motion are negligible during the pulsewidth. Thus, recast, thermal damage (microcracks), and heat-affected-zone (HAZ) are greatly reduced. The ablation depth of the femtosecond laser is on the order of 0.01 ~ 1 μm per pulse [45]. Hence, femtosecond laser ablation can be very precise.

The unique advantages make femtosecond lasers very promising for the fabrication of wide bandgap materials that is difficult for conventional tools. Femtosecond ablation of wide bandgap materials is the main interest of this paper. This is an active area with very significant scientific and engineering merits [11, 29, 46-49]. Bandgap is the energy difference between the top of the valence band and the bottom of the conduction band. There is no clear cutoff of bandgap to define wide bandgap materials. In this paper, wide-band materials refer to materials with a bandgap greater than 3 eV, including 1) some semiconductors, for example, ZnO (3.1 eV), SiC (3.0 ~ 3.25 eV), GaN (3.4 eV), and silicon nitride (3.9 ~ 4.1 eV), and 2) all dielectrics, for example, diamond (5.46 ~ 6.4 eV), AlN (6.2 eV), sodium chloride (7.5 eV), NaCl (8 eV), quartz (9 ~ 10 eV), silicon dioxide (9 eV), and sapphire (9.9 eV).

However, a typical femtosecond laser ablation is low throughput with high photon cost, which is not suitable for typical industrial applications [50]. Further, the underlying physical mechanism of femtosecond laser ablation remains very controversial and poorly understood [29, 51-53]. So far, all processes of

femtosecond laser ablation have been developed through a trial-and-error procedure without well-established theoretical models [16, 22, 32, 33, 45].

This paper reviews challenges in understanding energy transport during femtosecond laser ablation mainly for wide bandgap materials at the intensity on the order of 10^{13} ~ 10^{14} *W/cm*^{2}. Section 2 addresses different views of the photon absorption process. Avalanche ionization and multiphoton ionization are two major competing mechanisms that are considered for free electron generations in this section. After the critical density is created, the laser energy is absorbed mainly through inverse Brehmstrahlung and resonance absorption mechanism in a similar way as free electrons do in metals. Section 3 focuses on augments on the mechanisms of material removals that mostly occur after the pulse. Thermal vaporization and Coulomb explosion are two major mechanisms that are considered for material removals. Based on the discussions of energy transport, section 4 presents the estimation equations and unsolved problems for threshold fluence and ablation depth.

2. Femtosecond laser pulse energy absorption

The energy transport in femtosecond laser ablation can be separated into two stages: 1) photon energy absorption by electrons, and 2) absorbed energy redistribution to lattice leading to material removals [49, 54]. This stage separation is based on the assumption that ionization (few to tens of femtosecond) and free electron heating (during pulsewidth) complete in such a short time that the lattice temperature remains unchanged during the absorption of femtosecond pulse [55]. This section reviews the absorption of laser energy through ionization and free electron heating.

2.1. Basic concepts in absorption of femtosecond laser energy

Roughly, photon absorptions can be categorized into linear process and nonlinear process. Linear photon absorption obeys the **Beer-Lambert Law** [56], which states, "*The absorption of a specific wavelength transmitted through a material is a function of material path length and is independent of incident intensity*". At femtosecond pulsewidth, nonlinear absorption becomes significant for all materials, no mattering it is opaque or transparent to its wavelength. In femtosecond ablation, collisional impact ionization (avalanche ionization) and photoionization (multiphoton ionization and/or tunnel ionization) are major competing mechanisms for free electron generation [46, 57].

As shown in figure 1, if the kinetic energy of a free electron becomes sufficiently high by absorbing photons, part of the energy may transfer to a bound electron by collisions to overcome the ionization potential [58] and produce two free electrons, which is called **(collisional) impact ionization** [47]. Consequently, the free electrons absorb photons and produce more free electrons from the bound electrons. Such a series of the impact ionization process is called **avalanche ionization** [46], where free electron density exponentially increases. Avalanche ionization strongly depends on free electron density and is sometimes assumed as linearly proportional to laser intensity [59]. Its efficiency is determined by competitions between energy gain through inverse Bremsstrahlung and energy loss through phonon emission. Avalanche ionization is responsible for the ablation of wide bandgap materials at the laser intensities below 10^{12} *W/cm*^{2}.

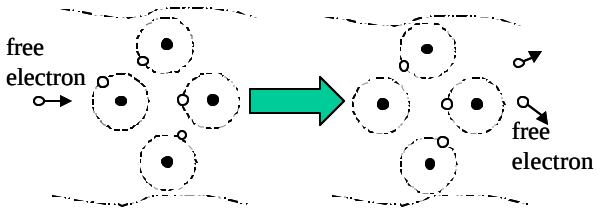

Figure 1. Collisional Impact ionization; avalanche ionization consists of a series of collisional impact ionizations

At high intensities (typically > 10^{13} *W/cm*^{2}) of femtosecond lasers, multiphoton ionization becomes significantly strong. As shown in figure 2, in a **multiphoton ionization** [60], several (*N*) photons with the energy of *hn* at the wavelength of *l* "simultaneously" strike a bound electron acting like a photon of *Nhn* at the wavelength of *l/N* due to very high photon flux (typically > 10^{31} cm^{-2}s^{-1}) of femtosecond lasers, i.e., a bound electron is freed from the valence band by absorbing several photons when the total energy of the absorbed photons is greater than the ionization potential [26, 38]. This absorption process is actually achieved through metastable quantum state(s). N-photon ionization is an Nth order process, and thus the cross section is very small at low intensities (< 10^{12} *W/cm*^{2}). Hence, only if laser intensity (photon flux) is very high, multiphoton ionization can be significant. At intensities above 10^{13} *W/cm*^{2}, multiphoton absorption becomes considerably strong and seed electrons are not required to initialize ionization in wide bandgap materials [61-64]. However, when intensities are higher than 10^{15} *W/cm*^{2}, tunnel ionization should be considered [29, 51, 59]. Tunnel ionization and multiphoton ionization belong to **photoionization** and sometimes

they are called **strong-electric-field ionization** [47, 65, 66]. Photoinization under femtosecond irradiation leads to metallic properties even for wide bandgap materials. Defects and impurities play a negligible role [67]. Since this paper is mainly interested in the laser intensities on the order of $10^{13} \sim 10^{14}$ *W/cm*^{2}, multiphoton ionization is our major interest instead of tunnel ionization.

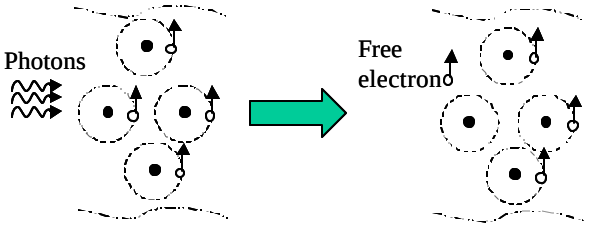

Figure 2. Multiphoton ionization

Laser ablation of a wide bandgap material is sometimes called **laser induced breakdown** in which the material is first transformed into absorbing plasma with metallic properties and subsequent laser-plasma interaction causes the phase changes of bulk materials [27, 30, 38, 49]. Buildup of free electrons is necessary to initialize the ablation. Free electron density is assumed to saturate at critical density**,** at which ablation occurs [59, 62, 68]. For femtosecond lasers, **critical density** is selected as the free electron density at which plasma oscillation frequency equals to the laser frequency:

$$n_{cr} = \frac{p\, m_e c^2}{e^2 l^2} \tag{1}$$

where m_e is the electron mass, c is the speed of light, e is the electron charge, and l is the laser wavelength. n_{cr} is about 0.98×10^{21} cm^{-3} for 1064 *nm* wavelength. At critical density, transparent wide bandgap materials become totally opaque. However, the selection of critical density using equation (1) is just a rough estimation. Gamaly et al., (2002) believe that when the ionization is completed, the free electron density is comparable to the ion density of about 10^{23} cm^{-3} for a 100 *fs*, 1064 *nm* laser [52]. Equation (1) shows that the critical density is independent of the pulsewidth, which is proven invalid by the experiments of Quéré et al. (2001) [48]. The relationship between critical density and pulsewidth should be clarified through analyzing the ionization mechanism, which remains a challenge.

2.2. Relative roles of avalanche ionization to multiphoton ionization

2.2.1. Multiphoton impact ionization. In femtosecond laser ablation of wide bandgap materials, the roles of multiphoton ionization and avalanche ionization in free electron generations are still controversial [27, 29, 49, 51-53, 64, 69). The early research on laser ablation of wide bandgap materials commonly assumed that avalanche ionization is responsible for the ablation [27, 70-73]. Recently, some researchers believe that, multiphoton ionization supplies seed electrons while avalanche ionization is still responsible for femtosecond ablation [32, 39, 46, 57, 59, 66, 69, 74, 75]. Perry et al. (2001) call this process **multiphoton impact ionization**. This opinion is in accord with the experiments of Du et al. (1994) [74] on the ablation of fused silica using 150 *fs* ~ 7 *ns*, 780 *nm* laser with the simplified analysis using the equation of Bloembergen (1974) [70].

Another evidence of multiphoton impact ionization is the experiments of Pronko et al. (1998) on the ablation of silicon using 80 *fs* ~ 9 *ns*, 786 *nm* ~ 1.06 *μm* lasers [46]. Their experiments show that the threshold of 1064 *nm* is always below that of 786 *nm.* Pronko et al., (1998) concluded that avalanche ionization still dominates the ablation [46], because in near IR range, longer wavelength radiation is more effective in producing avalanche ionization [76]. However, the wavelength dependence of the femtosecond ablation threshold is very controversial [32, 52, 57, 70, 76].

Perry, Stuart, and their colleagues developed well-known theories for multiphoton impact ionization based on kinetic equation and experiments on the ablation of dielectrics at 1053 *nm*, 852 *nm*, and 526 *nm* at the pulsewidth of 100 *fs* ~ 1 *ns* [51, 59, 62, 62]. In their theory, the free electron density distribution, $n_e(e, t)$, is described by the Fokker-Plank equation [51]:

$$\frac{\partial}{\partial e}\left[R_J(e,t)\,n_e(e,t) - g(e)E_p n_e(e,t) - D(e,t)\frac{\partial n_e(e,t)}{\partial e}\right] + \frac{\partial n_e(e,t)}{\partial t} = S(e,t) \tag{2}$$

where e is the electron kinetic energy, t is the time, $R_J(e, t)$ is the heating rate of electrons, $g(e)$ is the rate of electron-phonon energy transfer to the lattice, E_p is the energy of the typical phonon, $D(e, t)$ is the diffusion coefficient, and $S(e, t)$ is the source and sinks of electrons. The terms within the square bracket of equation (2) represent the electron distribution change because of Joule heating, $R_J(e,t)\,n_e(e,t)$, the inelastic scattering of phonon, $g(e)E_p n_e(e,t)$, and electron energy diffusion, $D(e,t)\frac{\partial n_e(e,t)}{\partial e}$. The heating rate of electrons is taken as:

$$R_J(e,t) = \frac{d(e)}{3}E^2(t) \tag{3}$$

where $E(t)$ is the electric field and $d(e)$ is the ac conductivity of an electron:

$$d(e) = \frac{e^2 t_m(e)}{m^*\left[1 + w^2 t_m^2(e)\right]} \quad (4)$$

where $1/t_m$ is the energy-dependent, electron-phonon transport scattering rate, m^* is the effective mass of an electron that is about the rest mass of an electron, and w is the laser frequency. The diffusion coefficient is given by:

$$D(e,t) = 2e R_J(e,t) \quad (5)$$

The term on the right of equation (2), $S(e, t)$, the source and sinks of electrons, includes the impact ionization term, $S_{imp}(e, t)$, and photoionization term, $S_{pi}(e, t)$.

$$\begin{aligned} S(e,t) &= S_{imp}(e,t) + S_{pi}(e,t) \\ &= 4n_e(2e + U_{IP}, t)\nu_I(2e + U_{IP}) \\ &\quad - n_e(e,t)\nu_I(e) + S_{pi}(e,t) \end{aligned} \quad (6)$$

where U_{IP} is the ionization potential and $n_I(e)$ is impact ionization rate described by the Keldysh impact formula [77]:

$$n_I(e) = c\left(\frac{e}{U_{PI}} - 1\right)^2 \quad (7)$$

where χ is a proportionality constant. The source term of impact ionization [51, 57, 59, 62, 63], and the source term of photoionization [57, 65, 78] in equation (6), have been extensively studied.

If energy deposited into electrons is much more than that to lattice during the pulse, a widely accepted simplified model is derived from equations (2) ~ (7) [51]:

$$\frac{dn_e(t)}{dt} = b(I)\, n_e(t) + P(I) \quad (8)$$

where $b(I)$ is the impact ionization term and $P(I)$ is the photoionization term. The loss term because of electron diffusion and recombination is neglected in equation (8). The solution to equation (8) is [59]:

$$n_e(t) = \left(\frac{P}{b} + n_{ini}\right)\exp(b\,t) - \frac{P}{b} \quad (9)$$

where n_{ini} is the initial electron density due to defects and impurities.

One of the major issues of this model is how to estimate impact ionization rate and photoionization rate. Stuart et al. (1996) [59] assume that 1) as soon as the kinetic energy of an electron reaches the critical energy, it produces another electron by impact ionization, and both electrons becomes zero kinetic energy, which is so-called "flux-doubling" condition and 2) the shape of electron distribution remains unchanged during the avalanche ionization. Under the two assumptions, at high laser intensities, avalanche rate can be assumed linearly proportional to laser intensity:

$$b = a_i I(t) \quad (10)$$

where a_i is a constant. In the case that the bandgap of the material is not too much greater than (4 times) the photon energy and there is no intermediate resonance, the photoionization rate can be expressed as a function of laser intensity [59]:

$$\mathrm{P(I)} = d_{\mathrm{N}} \left(\frac{\mathrm{I}}{\hbar w}\right)^N N_s \quad (11)$$

where d_N is the cross section of N-photon ionization with a unit of $cm^{2N}s^{N-1}$ that depends on the location of all other electrical states of the system, and N_s is the solid atom density. This model is limited to N ($\leq$ 4)-photon ionization without the consideration of tunnel ionization.

The result of equation (8) has been proven effective by comparing its results with the numerical solution of equation (2) [59]. Figure 3 shows that the avalanche ionization is mainly responsible for the ablation, while multiphoton ionization just supplies seed free electrons in the ablation of fused silica by a 100 *fs*, 1053 *nm* pulse at 10^{13} *W/cm*^{2}. Please note that the axis of electron density is logarithmic.

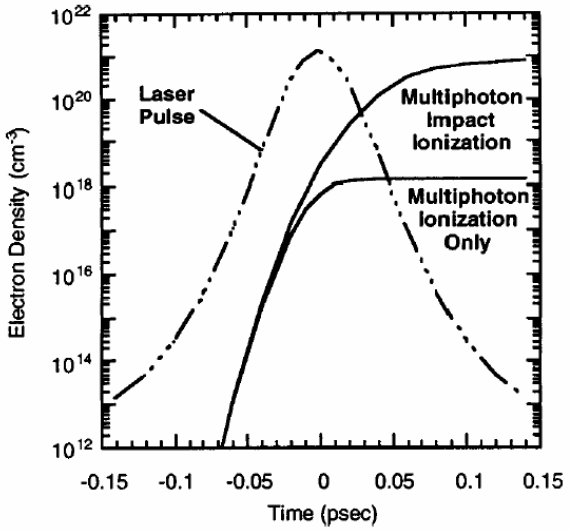

Figure 3. Calculated free electron density for the ablation of fused silica using a 100 *fs*, 1053 *nm* pulse at 10^{13} *W/cm*^{2} [62]

As shown in figure 4, the threshold predictions based on the flux-doubling model are in excellent agreements of their experiments [62]. The methodology used to estimate threshold is detailed in section 2.4. Although Perry's group assumes multiphoton impact ionization in their calculations [51, 59, 62, 63], the results demonstrate that at a pulsewidth shorter than 100 *fs*, the predicted threshold approaches the prediction by multiphoton ionization alone represented by dashed lines in figure 4 [62]. Multiphoton ionization alone

provides the electron critical density at extremely short 30 *fs* [51]. In this sense, the free electron generation dominated by multiphoton ionization can be considered as a specific case of the ablation by multiphoton impact ionization, where multiphoton ionization is so strong that the critical density is created before avalanche ionization significantly initializes.

But, the model of Stuart et al. (1995) [51] fails to explain the increase in threshold fluence with the decrease of pulse width (< 1 ps) [57]. Also, the model fails to interpret the incubations effects on ablation threshold of dielectrics as a function of the delay between dual beams [69, 79] Li et al. (1999) [69] add a decay term into the model to fit their experiment results:

$$\frac{dn_e}{dt} = a_i I(t) n_e + d_N \left(\frac{I}{\hbar w}\right)^N N_s - \frac{n_e}{t} \qquad (12)$$

where t is the decay time constant. However, this improvement is challenged by Petite et al. (1999) [79]. Petite et al. (1999) [79] explains the fast decay is as a consequence of the self-trapping, which disagrees with the assumption that seed electrons left by the first pulse contribute the avalanche ionization in the second beam.

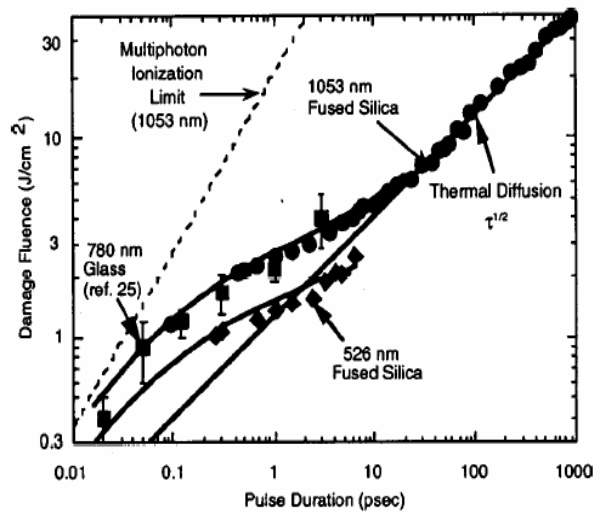

Figure 4. Ablation threshold of fused silica at different pulsewidths [62]

2.2.2. Thornber's model for avalanche rate and Keldysh's model for photoionization rate. As mentioned earlier, simplified methods of equations (10) and (11) for avalanche rate and photoionization rate are valid for very limited conditions. Thornber's model and Keldysh's theory can more precisely calculate the avalanche rate and photoionization rate respectively, which is valid for many more cases [57]. Thornber's model does not need the assumption of the linear proportionality between laser intensity and avalanche rate [57, 80]:

$$b(E) = \frac{v_s e E}{E_g} \exp\left(-\frac{E_I}{E(1+E/E_{phonon}) + E_{kT}}\right) \qquad (13)$$

where v_s is the saturation drift velocity (~ 2× 10^7 cm/s), E_g is the bandgap energy, E_I, E_{phonon}, and $E_{kT} \equiv E_I kT/E_g$ are the fields for carriers to overcome the decelerating effects of ionization scattering, optical phonon scattering, and thermal scattering in one mean free path respectively.

Keldysh's theory [77] can be used to calculate the photoionization rate as a function of the laser electric field with the consideration of tunnel ionization [57]:

$$P(E) = \frac{2w}{9p}\left(\frac{w\,m}{\sqrt{g_1}\hbar}\right)^{3/2} Q(g, x) \times \exp\left\{-p\,\langle x+1\rangle \frac{K_1(g_1) - E_2(g_1)}{E_2(g_2)}\right\} \qquad (14)$$

where w is laser frequency, m is the reduced mass of the electron and the hole:

$$m = \frac{m_e m_h}{m_e + m_h} \qquad (15)$$

where m_e is the mass of electron and m_h is the mass of the hole. In equation (14), γ is Keldysh's parameter in a solid,

$$g = \frac{w\sqrt{m E_g}}{eE} \qquad (16)$$

and,

$$g_1 = \frac{g^2}{1+g^2}, \qquad g_2 = 1 - g = \frac{1}{1+g^2} \qquad (17)$$

$$x = \frac{2}{p}\frac{E_g}{\hbar w}\frac{\sqrt{1+g^2}}{g} E_2\left(\frac{1}{1+g^2}\right) \qquad (18)$$

$$Q(g, x) = \sqrt{\frac{p}{2K_1(g_2)}} \times \sum_{n=0}^{\infty} \exp\left\{-np\,\frac{K_1(g_2) - E_2(g_2)}{E(g_1)}\right\} \Phi\left\{\frac{p}{2}\sqrt{\frac{(2\langle x+1\rangle - 2x + n)}{K_1(g_2)E_2(g_2)}}\right\} \qquad (19)$$

where K_1, E_2 are the complete elliptic integral of first kind and second kind respectively, <z> is the integer part of the number of z and,

$$\Phi(z) = \int_0^z \exp(y^2 - z^2)\,dy \qquad (20)$$

However, the prediction of Keldysh's model for multiphoton ionization is substantially higher than the measurements by Lenzner et al. (1998) [29] on the ablation of dielectrics using 5 ps ~ 5 fs and 780 nm lasers.

2.2.3. Probability form for ionization rates. To make the relative friction of avalanche ionization to

multiphoton ionization more clear, Gamaly et al. (2002) [52] express the free electron density as:

$$\frac{dn_e}{dt} = b\, n_e + p_{mpi} N_s \tag{21}$$

where N_s is solid atom density, b is the time dependent probability of impact ionization, and $p_{mpi} = P/N_s$, is the time dependent of probability of multiphoton ionization [26, 81, 82]. Gamaly et al. (2000) [52] estimate b and p_{mpi} by:

$$b = \frac{e_{osc}}{U_{PI}} \left(\frac{2w^2 n_{eff}}{w^2 + n_{eff}^2} \right) \tag{22}$$

$$p_{mpi} = w N^{3/2} \left(\frac{e_{osc}}{2U_{PI}} \right)^N \tag{23}$$

where e_{osc} is the electron quiver (oscillation) energy in the laser field, N is the minimum number of photons needed to overcome the bandgap in multiphoton ionization, and n_{eff} is the effective collision frequency. Equations (22) and (23) show that the relative role of avalanche ionization to multiphoton ionization significantly depends on the electron quiver energy and ionization potential. If $e_{osc} > U_{PI}$, multiphoton ionization dominates the process. Oscillation energy, e_{osc} , in the unit of eV, is expressed in a scaling form [52]:

$$e_{osc} = 9.3(1 + a_{pol}^2) \frac{I}{10^{14}} l^2 \tag{24}$$

where a_{pol} is the coefficient for the beam polarization: for the circular, a_{pol} =1 and for the linear polarization, a_{pol} =0, I is in the unit of W/cm^2, and l is in the unit of mm.

If laser intensity is greater than 10^{14} W/cm^2, it is obvious that $e_{osc} > U_{PI}$ and multiphoton ionization dominates for most materials. For instance, silicon ablated by 1064 nm and 100 fs pulse at 2×10^{13} W/cm^2, avalanche ionization is responsible for the ablation, while at 10^{14} W/cm^2 multiphoton ionization dominates the process [52]. The predication of Gamaly et al. (2002) [52] is supported with the recent experiments on imaging femtosecond laser-induced electronic excitation in glass by Mao et al. (2003) [64]. They measured the evolution of laser-induced electronic plasma using a femtosecond time-resolved imaging technique at the intensity range of $5\times10^{12} \sim 10^{14}$ W/cm^2.

2.2.4. Ablation dominated by multiphoton ionization. In the latest three years, some researchers [47-49] discovered that multiphoton ionization actually dominates absorption at the laser intensities on the order of 10^{14} W/cm^2. Using a frequency-domain interferometry to measure the relative phase of the reference and probe beams, Quéré et al. (2001) [49] discovered no sign of avalanche ionization in the ablation of SiO_2 (bandgap, 9.0 eV), Al_2O_3 (8.8 eV), and MgO (7.65 eV), by a 790 nm, 60 fs laser. They concluded that multiphoton ionization dominates in femtosecond laser ablation of dielectrics. Using the time dependent Boltzman equation, Kaiser et al. (2000) [47] demonstrate that at a laser electric field of 150 MV/cm, avalanche ionization is of minor importance for laser pulsewidths below 100 fs and only at pulsewidths above 200 fs avalanche ionization becomes as important as multiphoton ionization, as shown in figure 5.

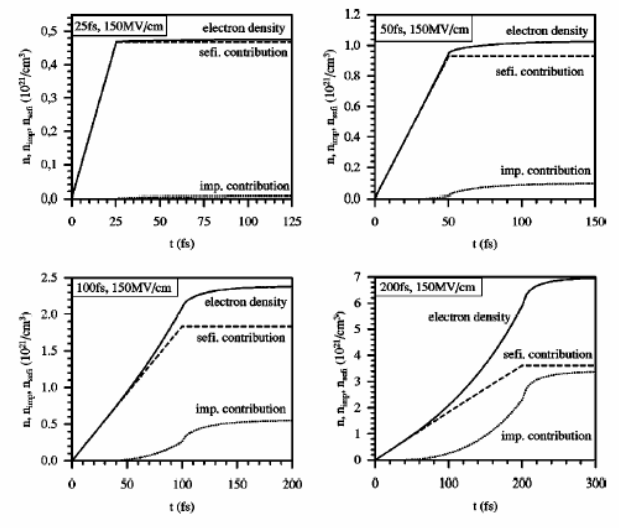

Figure 5. Time dependent of free electron contribution by avalanche ionization (impact ionization presented as imp.) and photoionization (strong-electric-field ionization presented as sefi.) at 150 MV/cm with different pulsewidths [47]

2.3. Electron heating

At intensities above 10^{14} W/cm^2, it takes just a few femtoseconds to reach the critical electron density by ionizations under femtosecond pulse [52]. After the critical density is created, the laser energy is absorbed mainly through inverse Brehmstrahlung and resonance absorption mechanism [53, 83, 84, 85] in a similar way as free electrons do in metals. The refractive index can be calculated by [52]:

$$r = \sqrt{\frac{w_{pe}}{2w} \left(1 + \frac{w^2}{w_{pe}^2} \right)^{-1}} \tag{25}$$

where w_{pe} is electron plasma frequency. Please note that Gamaly et al. (2002) [52] believe that the electron plasma density near the ablation threshold is greater than laser density, which is different with the assumption for critical density in section 2.1. The absorption coefficient can be estimated by Fresnel formula [86]:

$$a = \frac{4r}{(1+r)^2 + r^2} \tag{26}$$

During femtosecond pulse duration, electrons have no time to transfer energy to ions or out of the bulk material. Most of the pulse energy is first deposited into electrons in a small depth by the laser electric field. The laser electric field can be found as a solution to a Maxell equation coupled to the material equation. The solution is straightforward when the material parameters are constant in time and space and independent on the incident intensity. In this case, the interaction falls into the framework of well-known skin effects. The skin layer can be estimated by:

$$l_s \approx a \frac{c}{2w}\left(1 + \frac{1}{r} + \frac{1}{2r^2}\right) \tag{27}$$

Electron conduction time, t_h, can be calculated by [87]:

$$t_h = \frac{l_s^2}{k} = \frac{3l_s^2}{l_e v_e} \tag{28}$$

where k is the coefficient of thermal diffusion; l_e and v_e are electron free mean paths and velocity respectively; the energy conservation of the electron energy in the process is described as [88]:

$$c_e(T_e) n_e \frac{\partial T_e}{\partial t} = -\frac{\partial Q}{\partial z} \tag{29}$$

where c_e is the specific heat of free electrons; Q is the absorbed energy flux in the skin layer:

$$Q = a\, I \exp\left(-\frac{2z}{l_s}\right) \tag{30}$$

where a is the absorption coefficient. The solution to the equation (29) is simple with the assumptions of that free electron density, n_e, absorption coefficient, α, and skin layer, l_s, are all time independent. However, all the three quantities are actually the functions of the laser intensity and time, which reduces the effectiveness of the skin-layer model. Further, free electrons are not in equilibrium states, which were demonstrated by experiments [89, 90]. Hence, it is imprecise to use the equilibrium temperature to describe electrons [91]. Rethfeld et al. (2002) [25] investigated the non-equilibrium dynamics of the electrons in femtosecond laser ablation of metals using a full Boltzmann collision integral that is free of phenomenological parameters. They found that the laser energy absorption is well described by a plasma-like absorption term after the critical density is created.

3. Material removal mechanisms

The dissipation of the absorbed energy in bulk material and the corresponding material removals take place mostly after pulse duration, which also remains poorly understood and has many different views [40, 92-103]. Among the views, two major mechanisms have been extensively discussed: 1) **thermal vaporization** [93, 94, 98] where the electron-phonon collisions increase the local temperature above the vaporization point. 2) **Coulomb explosion** [40, 97, 99-103] where excited electrons escape from the bulk materials and form a strong electric field that pulls out the ions within the impact area. According to these two mechanisms of material removals, femtosecond laser ablation can be divided into two regimes [104-106]: 1) **strong ablation** dominated by thermal vaporization at intensities significantly higher than the ablation threshold and 2) **gentle ablation** governed by the Coulomb explosion near the ablation threshold.

3.1. Thermal vaporization (strong ablation)

Compared with the Coulomb explosion, characteristics of thermal vaporization (strong ablation) include [44, 97, 100, 104, 105, 106, 107]: 1) emitted species are likely to have the similar kinetic energy; 2) temperatures of emitted species are near the vaporization point; 3) the temperature of the interface in bulk material side is near the vaporization point during the ablation process; 4) volume of removal material per pulse is on the order of submicrometer; and 5) ablated surface is rough.

Ladieu et al., (2002) [49] measured heating and estimated the local temperature of the crafter on a quartz sample at miliseconds after the sample is ablated by 50 *fs* and 790 *nm* laser at 1 ~ 6 times of threshold fluence. They found temperatures above 3000°C even at the fluence close to threshold after a virtually infinite time (several milliseconds) with respect to pulsewidth of 50 *fs*. Hence, they concluded that thermal vaporization dominates the material removals in a whole fluence regime of 1 ~ 6 times of threshold fluence. Schmidt et al. (2000) [108] observed that desorption of metals (Al, Ag, Fe, and Ni) by an 800 *nm*, 30 *fs* laser at 10 ~ 50 mJ/cm^2 using interferometric time-resolved pump-probe measurements. They concluded that thermal vaporization is mainly responsible for the ablation, while Coulomb explosion is insignificant due to effective electron screening in metals. This conclusion is supported by the experiments on ablation of metals (Au) and semiconductors (Si) by 800 *nm*, 200 *fs* laser at 4 J/cm^2 [107]. Stoian et al. (2002) believe that the Coulomb explosion is not a major mechanism in the ablation of Au and Si in their experiments [107]. In semiconductors and metals, electron mobility is high, which enhances electron screening at supercritical electron density. Electron screening reduces the accumulation of positive charge during the femtosecond laser pulse, and then reduces the electric field, which reduces the effectiveness of the Coulomb explosion.

3.2. Coulomb explosion (gentle ablation)

Compared with thermal vaporization, characteristics of the Coulomb explosion (gentle ablation) include [93, 94, 96, 97, 104-106]: 1) ions of different materials have similar momenta; 2) majority of ions is much faster than those in thermal vaporization; 3) volume of removal materials is on the order of tens of nanometers; 4) the ablated surface tends to be smooth and material removal is accurately controllable on the *nm* scale; and 5) there are two distinct velocity regimes of electrons: prompt electrons with energy order of *eV* and slow electrons with energy order of *meV*. Slow electrons actually are trapped by positive ions [107].

Figure 6 shows the time-of-flight mass spectrometer of emitted materials from Al_2O_3 by 200 *fs*, 800 *nm* laser at 4 J/cm^2 [107]. The characteristics of the Coulomb explosion are very obvious: slow electrons and ions in figure 6 (a), and prompt electrons in figure 6 (b). Please note the different time scales in two sub figures. The slow electrons can be considered as plasma electrons. Using time-of-flight and emission spectroscopy measurement, Ye and Grigoropoulos (2001) [109] found the kinetic energy of titanium ions can reach up to 3 ~ 10 *keV* ablated by 800 *nm*, 80 *fs* laser at 1.25×10^{13} W/cm^2, which demonstrates that the Coulomb explosion is the mechanism of the material removal.

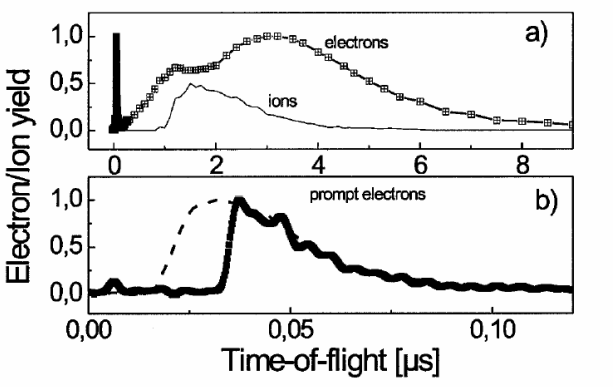

Figure 6. Electron and ion time-of-flight data of Al_2O_3 by a 200 *fs*, 800 *nm* laser at 4 J/cm^2. Squares (thick line): from Al_2O_3 and dashed line from Al [107]

The magnitude of the electric field formed in the Coulomb explosion depends on the electron kinetic energy and the gradient of electron density along the normal to the target materials [87]:

$$E_a = -\frac{e(t)}{e}\frac{\partial \ln n_e}{\partial z} \qquad (31)$$

This electric field consequently pulls ions out of the bulk materials if its magnitude is high enough. The electrostatic force of this field on the ions, F_{st}, can be calculated by, $F_{st}=eE_a$. Another force on the ions by the electric field is the ponderomotive force due to the gradient of the electric field that is estimated by [110]:

$$F_{pf} = -\frac{2p\,e^2}{m_e c w^2}\nabla I \approx \frac{I}{2n_e c l_s}\frac{w_{pe}^2}{w^2} \qquad (32)$$

where w is laser frequency; w_{pe} is the electron plasma frequency; m_e is the mass of electron. However, ponderomotive force is much smaller than the electronic force [52] and can be ignored.

3.3. Transitions between thermal vaporization and Coulomb explosion

Actually, the two competing mechanisms may coexist in material removals. The particular mechanism depends on material properties, laser intensity (duration), wavelength, and number of pulses [44]. As shown in figure 7, Stoian et al. (2000) [100] identified that in the initial several pulses the Coulomb explosion dominates material removals of crystalline Al_2O_3 by an 800 *nm*, 100 *fs* laser at fluence slightly above the threshold, where different ions have similar momenta and kinetic energy is high. After a certain incubation period, the material removals gradually switch to thermal vaporization. At a large number of pulses (>100), thermal vaporization dominates the material removals, where different ions have similar kinetic energy and kinetic energy of ion is relatively low. Although the characteristics of thermal vaporization and Coulomb explosion seem obvious, it is a big challenge to theoretically predict the relative roles of two competing mechanisms in material removals.

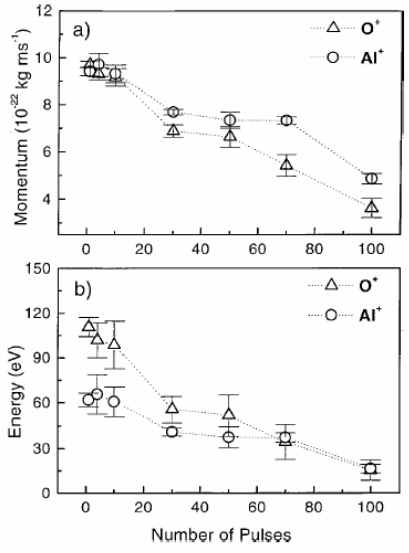

Figure 7. Momentum and energy of ions under different pulses [100]

4. Threshold fluence and ablation depth

On the basis of the previous discussion of the fundamental mechanisms in the femtosecond ablation, this section discusses the methodologies to estimate threshold fluence and ablation depth.

4.1. Threshold fluence

Laser ablation of wide bandgap materials exhibits threshold behaviors: ablation happens only when the fluence is higher than a certain value at a given pulsewidth. Jeschke et al. (2001) defined the ablation **threshold fluence** as *"the laser fluence at which lattice instabilities of such magnitude are induced that the system is irreversibly damaged and at least a mono-layer of material is removed"* [111]. In experiments, threshold fluence is actually determined by visual acquisition [59], ablation depth measurement [29], or plasma radiation monitoring [69].

A significant characteristic of femtosecond ablation of dielectrics is that its threshold fluence is higher than the prediction of the law of the square root of the pulsewidth [29, 74]. This can be briefly explained as follows:

In ionization-dominated ablations by femtosecond pulses, the electron temperature dominates the electron-phonon temperature. Thus, photon absorption depth instead of the thermal diffusion depth governs the heated volume. Thermal diffusion depth is linearly proportional to the square of pulsewidth, while photon absorption depth is not. Hence, threshold fluence of femtosecond lasers deviates from the law of the square root of the pulsewidth that is valid for long pulses.

It is widely assumed that ablation starts when the free electron density reaches the critical density [51, 74]. According to this assumption, threshold fluence can be considered as the minimal fluence to create the critical density. Based on this assumption, the theoretical threshold logarithmically depends on the value of critical density [59]:

$$F_{th} = \frac{2}{a}\ln\left(\frac{n_{cr}}{n_0}\right) \qquad (33)$$

where n_0 is the seed electrons generated by multiphoton ionization:

$$n_0 = \int_0^{\infty} P(I)dt \qquad (34)$$

As shown in figure 4, the threshold predictions based on the model of Perry's group are in excellent agreement of their experiments [59, 62].

From the viewpoint of material removal mechanisms, for the Coulomb explosion, it is assumed that threshold fluence is the minimal fluence to create an electric field high enough for electrons to overcome the sum of the binding energy of ions in the lattice, e_b, and ionization potential, U_{PI}. Under this assumption, the threshold fluence of wide bandgap materials can be expressed as [52]:

$$F_{th} = \frac{3}{4}\left(e_b + U_{PI}\right)\frac{l_s n_e}{a} \qquad (35)$$

Equations (33) and (35) present only conceptual estimation methodologies that are by no means mature. Still, there remain many challenges regarding threshold fluence for the femtosecond laser ablation for future research:

1. The wavelength dependence of femtosecond ablation threshold remains very controversial. If the wavelength is decreased, there are four different opinions on the corresponding changes of the threshold fluence:
   - Unchanging [111], because molecular dynamics simulations based on microscopic electronic theory show that ablation thresholds are nearly independent of the pulsewidth in the range of 10 ~ 500 *f*s.
   - decreasing [52], which is based on analytic equations.
   - unchanging, if avalanche ionization dominates; or decreasing, if multiphoton ionization dominates [57, 70].
   - increasing if avalanche ionization dominates; or decreasing, if multiphoton ionization dominates. [46, 76].

   Hence, this challenge is closely related to the roles of multiphoton ionization and avalanche ionization.
2. Incubation effects on femtosecond threshold fluence [27, 29, 69] remain poorly understood. Incubation increases multiphoton absorption coefficient by an order of magnitude [67]. Figure 8 shows that in femtosecond dual beam ablation, even at picosecond delays, the second pulse threshold is still below that of the first pulse [69]. The fitting in figure 8 is based on equation (9). The accumulation of electrons by incubation alone cannot explain this phenomenon. The material modification might also contribute to the incubation. Petite et al. (1999) [79] argue that the self-trapping mechanism must be taken into consideration for incubation.

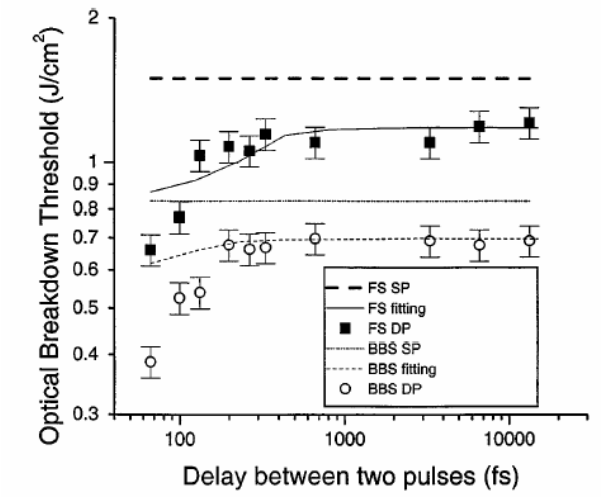

Figure 8. Threshold fluence of single pulse (SP) and double pulse (DP) for fused silica (FS) (bandgap» 9 eV) and Barium Aluminum Borosilicate (BBS bandgap» 4 eV) [69]

4.2. Ablation depth

Ablation depth is governed by photon absorption depth that is typically longer than thermal diffusion depth during a femtosecond pulse. It is assumed that the actual fluence at the ablation depth, d, equals to absorbed threshold fluence, $F(z=d)=(1-r)F_{th}$ [112]. Based on this assumption, the ablation depth can be estimated by [112]:

$$d = \frac{1}{a}\ln\left(\frac{F}{F_{th}}\right) \tag{36}$$

where F is the laser fluence. The assumption of that reflectivity is constant seems invalid during the femtosecond laser ablation process [39]. The ablation depth of a femtosecond pulse can be approximated by the skin-effect model [52]:

$$d = \frac{l_s}{2}\ln\frac{F}{F_{th}} \tag{37}$$

This estimation is very rough, which obviously needs future improvements.

Another assumption for the ablation depth is that the free electron density at the ablation depth equals to critical density. Based on this assumption, the model of Stuart et al. (1996) can be used to discuss the ablation-depth dependence on pulsewidth. Refer to equations (8), (10), and (11), if avalanche ionization dominates photon absorption, electron density (thus, ablation depth) is independent of pulsewidth at a fixed fluence. By contrast, if multiphoton ionization dominates photon absorption, electron density (thus, ablation depth) is expected to rapidly decrease with decrease of pulsewidth at a fixed fluence [29]. This presents an approach to determine the ionization mechanism of free electron generations during femtosecond laser ablation.

5. Summary and conclusions

Irradiated under a femtosecond pulse, the impact area of a wide bandgap material is first transformed into absorbing plasma with metallic properties and the subsequent laser-plasma interaction causes the phase changes of bulk materials. The major conclusions and unsolved problems regarding energy transport during femtosecond laser ablation of wide bandgap materials are summarized as follows:

1. Free electrons are generated by ionization and saturate at critical density. The actual relationship between critical density and pulsewidth should be clarified through analyzing the ionization mechanism. However, the ionization mechanism remains controversial. Some researchers believe that multiphoton ionization supplies seed electrons, while avalanche ionization is still responsible for the ablation. However, as the pulsewidth becomes below 100 *fs*, the ionization approaches to the regime dominated by multiphoton ionization. Some other research based on analytic models, Boltzman equations, and experimental measurements, concluded that multiphoton ionization does dominate free electron generation at the intensities > 10^{14} *W/cm*^{2}. As for modeling, the flux-doubling model is in excellent agreement with some experiment results, but it fails to explain the increase in threshold fluence with the decrease of femtosecond pulsewidth and the incubation effects on threshold fluence. On the other hand, the prediction of Keldysh's model for multiphoton ionization is substantially higher than the measurements.
2. After the critical density is created, the laser energy is absorbed mainly through inverse Brehmstrahlung and the resonance absorption mechanism. Free electrons are not in equilibrium states in the electron heating process during the pulsewidth. Also, free electron density, absorption coefficient, and skin layer length are all time dependent and intensity dependent. Strictly speaking, these facts make the skin-effect model invalid to hardly describe the electron heating process.
3. Mechanisms of material removals by femtosecond laser also remain controversial. The particular mechanism strongly depends on material properties, laser intensity (duration), wavelength, and number of pulses. A strong ablation regime is dominated by thermal

vaporization often at intensities considerably higher than threshold fluence. Gentle ablation regime is governed by the Coulomb explosion at intensities near the ablation threshold fluence in dielectrics. Incubation and electron screening can significantly reduce the probability of Coulomb explosion. However, it remains a challenge to predict the roles of thermal vaporization and Coulomb explosion, which is critical for ablation modeling.

4. Ablation wavelength dependence of femtosecond threshold fluence remains very controversial. Further, so far incubation effects on threshold fluence cannot be well explained.
5. The ablation depth of the femtosecond laser is governed by photon absorption depth. It is assumed that at the ablation depth, the fluence equals to absorbed threshold fluence or free electron density equals to critical density. The estimations based on the assumptions are very rough, which obviously needs future improvements.

6. Acknowledgements

This work was supported partially by the US Amy Research Office under Grant No. DAAG55-98-1-0097 and NSF under Grant No. 0116158.

7. References

[1] S. Preuss, A. Demchuk, and M. Stuke, "Sub-picosecond UV laser ablation of metals", *Appl. Phys. A*, 1995, **61**, 1, pp. 33-37.

[2] T. Götz and M. Stuke, "Short-pulse UV laser ablation of solid and liquid metals: indium", *Appl. Phys. A*, 1997, **64**, 6, pp. 539-543.

[3] M. Feuerhake, J.H. Klein-Wiele, G. Marowsky, and P. Simon, "Dynamic ablation studies of sub-micron gratings on metals with sub-picosecond time resolution", *Appl. Phys. A*, 1998, **67**, 5, pp. 603-606.

[4] K. Furusawa, K. Takahashi, H. Kumagai, K. Midorikawa, and M. Obara, "Ablation characteristics of Au, Ag, and Cu metals using a femtosecond Ti:sapphire laser", *Appl. Phys. A*, 1999, **69**, 7, pp. S359-S366.

[5] S. Küper and M. Stuke, "Ablation of polytetrafluoroethylene (Teflon) with femtosecond UV excimer laser pulses", *Appl. Phys. Lett.*, **54**, 1, 1989, pp. 4-6

[6] S. Baudach, J. Bonse, and W. Kautek, "Ablation experiments on polyimide with femtosecond laser pulses", *Appl. Phys. A*, 1999, **69**, 7, pp. S395-S398.

[7] P. Simon and J. Ihlemann, "Machining of submicron structures on metals and semiconductors by ultrashort UV-laser pulses", *Appl. Phys. B*, 1995, **63**, 5, pp. 505-508.

[8] G. Herbst, M. Steiner, G. Marowsky, and E. Matthias, "Ablation of Si and Ge using UV femtosecond laser pulses", *Mater. Res. Soc. Symp. Proc*., 1996, **397**, pp. 69-74.

[9] K. Chen, J. Ihlemann, P. Simon, I. Baumann, and W. Sohler, "Generation of submicron surface gratings on $LiNbO_3$ by ultrashort UV laser pulses", *Appl. Phys. A*, 1997, **65**, 4-5, pp. 517-518.

[10] G. Dumitru, V. Romano, H.P. Weber, M. Sentis, and W. Marine, "Femtosecond ablation of ultrahard materials", *Appl. Phys. A*, 2001, **74**, 6, pp. 729-739.

[11] K. Kawamura, T. Ogawa, N. Sarukura, M. Hirano, and H. Hosono, "Fabrication of surface relief gratings on transparent dielectric materials by two-beam holographic method using infrared femtosecond laser pulses", *Appl. Phys. B*, 2000, **71**, 1, pp 119-121.

[12] F. Korte, J. Koch, S. Nolte, C. Fallnich, A. Ostendorf, and B.N. Chichkov, "Nanostructuring of metal layers and transparent materials with femtosecond laser pulses", *ICALEO 2002*, October 14-17, 2002, Scottsdale, Arizona.

[13] H. Loesel, J.P. Fischer, M.H. Götz, C. Horvath, T. Juhasz, F. Noack, N. Suhm, and J.F. Bille, "Non-thermal ablation of neural tissue with femtosecond laser pulses", *Appl. Phys. B*, 1998, **66**, 1, pp. 121-128.

[14] M Bao and W. Wang, "Future of microelectromechanical systems", *Sensors & Actuators A*, 1996, **56**, pp. 135-141.

[15] J. Fluiman, "Microsystem technology objective", *Sensor & Actuators A*, 1996, **56**, pp.151-166.

[16] B.N. Chichkov, C. Momma, S. Nolte, F. von Alvensleben, and A. Tünnermann, "Femtosecond, picosecond and nanosecond laser ablation of solids", *Appl. Phys. A*, 1996, **63**, 2, pp. 109-115.

[17] A.S. Holmes, "Laser fabrication and assembly processes for MEMS", *SPIE Photonics West LASE2001*, January 19-26, 2001, San Jose, Calif.

[18] A.S. Holmes and S.M. Saidam, "Sacrificial layer process with laser-driven release for batch assembly operations", *J. Microelectromech. Syst.*, 1998, **7**, pp. 416-422.

[19] V.P. Veiko, "Laser microshaping, fundamentals, practical applications, and future prospect", *RIKEN Review*, 2001, **32**, pp. 11-18.

[20] Y.F. Lu, Y. Zhang, and W.D. Song, "Laser cleaning of tiny particles in a thin liquid layer and it's theoretical model", *Appl. Surf. Sci*., 1999, **139**, pp. 140-144.

[21] P. Simon, J. Bekesi, C. Dölle, J.H. Klein-Wiele, G. Marowsky, S. Szatmari, and B. Wellegehausen, "Ultraviolet femtosecond pulses: key technology for sub-micron machining and efficient XUV pulse generation", *Appl. Phys. A*, 2002, **74**, 9, pp. S189-S192.

[22] S. Banks, L. Dinh, B.C. Stuart, M.D. Feit, A.M. Komashko, A.M. Rubenchik, M.D. Perry, and W. McLean, "Short-pulse laser deposition of diamond-like carbon thin films", *Appl. Phys. A*, 1999b, **69**, 7, pp. S347-S353.

[23] P.S. Banks, M.D. Feit, A.M. Rubenchik, B.C. Stuart, and M.D. Perry , "Material effects in ultra-short pulse laser drilling of metals", *Appl. Phys. A*, 1999a, **69**, 7, pp. S377-S380.

[24] A.V. Lugovskoy and I. Bray, "Ultrafast electron dynamics in metals under laser irradiation", *Phys. Rev. B*, 1999, **60**, pp. 3279-3288.

[25] B. Rethfeld, A. Kaiser, M. Vicanek, and G. Simon, "Ultrafast dynamics of nonequilibrium electrons in metals under femtosecond laser irradiation", *Phys. Rev. B*, 2002, 65, pp. 214303~ 214313.

[26] Y.A. Il'insky and L.V. Keldysh, *Electromagnetic response of material media*, Plenum, New York, 1994.

[27] S.C. Jones, P. Braunlich, R.T. Casper, X.A. Shen, and P. Kelly, "Recent progress on laser-induced modifications and intrinsic bulk damage of wide-gap optical materials", *Opt. Eng*., 1989, **28**, pp. 1039-1068.

[28] M.H. Niemz, "Threshold dependence of laser-induced optical breakdown on pulse duration", *Appl. Phys. Lett*., 1995, **66**, pp. 1181-1183.

[29] M. Lenzner, J. Krüger, S. Sartania, Z. Cheng, C. Spielmann, G. Mourou, W. Kautek, and F. Krausz, "Femtosecond optical breakdown in dielectrics", *Phys. Rev. Lett.*, 1998, **80**, pp. 4076–4079.

[30] D.V. Linde and H. Schüler, "Breakdown threshold and plasma formation in femtosecond laser-solid interaction", *J. Opt. Soc. Am. B*, 1996, **13**, pp. 216-223.

[31] F.H. Loesel, M.H. Niemz, J.F. Bille, and T. Juhasz, "Laser-induced optical breakdown on hard and soft tissues and its dependence on the pulse duration: experiment and model", *IEEE J. Quant. Electron*, 1996, **32**, pp. 1717-1722.

[32] P.P. Pronko, S.K. Dutta, D. Du, and R.K. Singh, "Thermophysical effects in laser processing of materials with picosecond and femtosecond pulses", *J. App. Phys.*, 1995, **78**, 10, pp. 6233-6240.

[33] B.N. Chichkov, A. Ostendorf, F. Korte, and S. Nolte, "Femtosecond laser ablation and nanostructuring", *ICALEO 2001*, October 15-18, 2001, Jacksonville, Florida.

[34] J.G. Fujimoto, J.M. Liu, E.P. Ippen, and N. Bloembergen, "Femtosecond laser interaction with metallic tungsten and nonequilibrium electron and lattice temperatures", *Phys. Rev. Lett*., 1984, **53**, pp. 1837-1840.

[35] H.E. Elsayed-Ali, T.B. Norris, M.A. Pessot, and G.A. Mourou, "Time-resolved observation of electron-phonon relaxation in copper", *Phys. Rev. Lett*., 1987, **58**, pp. 1212-1215.

[36] R.W. Schoenlein, W.Z. Lin, J.G. Fujimoto, and G.L. Eesley, "Femtosecond studies of nonequilibrium electronic processes in metals", *Phys. Rev. Lett*., 1987, **58**, pp. 1680-1683.

[37] S.D. Brorson, A. Kazeroonian, J.S. Moodera, D.W. Face, T.K. Cheng, E.P. Ippen, M.S. Dresselhaus, and G. Dresselhaus, "Femtosecond room-temperature measurement of the electron-phonon coupling constant gamma in metallic superconductors", *Phys. Rev. Lett*., 1990, **64**, pp. 2172-2175.

[38] X. Liu, D. Du, and G. Mourou, "Laser ablation and micromachining with ultrashort laser pulse", *IEEE J of Quant. Elect*., 1997, **33**, pp. 1706-1716.

[39] M.D. Shirk and P.A. Molian, "A review of ultrashort pulsed laser ablation of materials", *J Laser Appl*., 1998, **10**, pp. 18-28.

[40] X. Wang and X. Xu, "Molecular dynamics simulation of heat transfer and phase change during laser material interactions", *J. Heat Transfer*, 2002, **124**, pp. 265-274.

[41] C.D. Decker, W.B. Mori, J.M. Dawson, and T. Katsouleas, "Nonlinear collisional absorption in laser-driven plasmas", *Phys. Plasmas*, 1994, **1**, pp. 4043-4049.

[42] E. Bésuelle, R.R.E. Salomaa, and D. Teychenné, "Coulomb logarithm in femtosecond-laser–matter interaction", *Phys. Rev. E*, 1999, **60**, pp. 2260-2263.

[43] Q.L. Dong, J. Zhang, and H. Teng, "Absorption of femtosecond laser pulses in interaction with solid targets", *Phys. Rev. E*, 2001, **64**, pp. 026411-026416.

[44] K. Sokolowski-Tinten, J. Bialkowski, A. Cavalleri, D. von der Linde, A. Oparin, J. Meyer-ter-Vehn, and S. I. Anisimov, "Transient states of matter during short pulse laser ablation", *Phys. Rev. Lett*., 1998a, **81**, pp. 224-227.

[45] B. Wolff-Rottke, J. Ihlemann, H. Schmidt, and A. Scholl, "Influence of the laser-spot diameter on

photo-ablation rates", *Appl. Phys. A*, 1995, **60**, 1, pp. 13-17.

[46] P.P. Pronko, P. VanRompay, A. Horvath, C.F. Loesel, T. Juhasz, X. Liu, and G. Mourou, "Avalanche ionization and dielectric breakdown in silicon with ultrafast laser pulses", *Phys. Rev. B*, 1998, **58**, pp. 2387-2390.

[47] A. Kaiser, B. Rethfeld, M. Vicanek, and G. Simon, "Microscopic processes in dielectrics under irradiation by subpicosecond laser pulses", *Phys. Rev. B*, 2000, **61**, pp. 11437-11450.

[48] F. Quéré, S. Guizard, and P. Martin, "Time-resolved study of laser-induced breakdown in dielectrics", *Europhys. Lett.*, 2001, **56**, 1, pp. 138-144.

[49] F. Ladieu, P. Martin, and S. Guizard, "Measuring thermal effects in femtosecond laser-induced breakdown of dielectrics", *Appl. Phys. Lett.*, 2002, **81**, pp. 957-959.

[50] J. Machan, M. Valley, G. Holleman, M. Mitchell, D. Burchman, J. Zamel, G. Harpole, H. Injeyyan, and L. Marabella, "Diode-pumped Nd:YAG laser for precision laser machining", *J. Laser Appl.*, 1996, **8**, pp. 225-232.

[51] B.C. Stuart, M.D. Feit, A.M. Rubenchik, B.W. Shore, and M.D. Perry, "Laser-induced damage in dielectrics with nanosecond to subpicosecond pulses", *Phys. Rev. Lett.*, 1995, **74**, pp. 2248-2251.

[52] E.G. Gamaly, A.V. Rode, B. Luther-Davies, and V.T. Tikhonchuk, "Ablation of solids by femtosecond lasers: ablation mechanism and ablation thresholds for metals and dielectrics", *Phys. of Plas.*, 2002, **9**, pp. 949-957.

[53] V. Rode, B. Luther-Davies, and E.G. Gamaly, "Ultrafast ablation with high-pulse-rate lasers part I: theoretical considerations", *J. Appl. Phys.*, 1999, **85**, pp. 4213-4221.

[54] J.C. Diels and W. Rudolph, *Ultrashort Laser Pulse Phenomena*, Academic Press, 1996.

[55] P. Gibbon, and E. Forster, "Short-pulse laser-plasma interactions", *Plasma Phys. Control Fusion*, 1996, **38**, pp. 769-793.

[56] S.S. Li, *Semiconductor Physical Electronics*, Plenum, New York, 1993.

[57] A. Tien, S. Backus, H. Kapteyn, M. Murnane, and G. Mourou, "Short-pulse laser damage in transparent materials as a function of pulse duration", *Phys. Rev. Lett.*, 1999, **82**, pp. 3883-3886.

[58] K. Wong, S. Vongehr, and V.V. Kresin, "Work functions, ionization potentials, and in between: scaling relations based on the image-charge model", *Phys. Rev. B*, 2003, **67**, pp. 035406-035414.

[59] B. C. Stuart, M. D. Feit, S. Herman, A. M. Rubenchik, B. W. Shore, and M. D. Perry, "Nanosecond-to-femtosecond laser-induced breakdown in dielectrics," *Phys. Rev. B*, 1996, **53**, pp. 1749-1761.

[60] S. Guy, M.F. Joubert, B. Jacquier, and M. Bouazaoui, "Excited-state absorption in $BaY_2F_8:Nd^{3+}$", *Phys. Rev. B*, 1993, **47**, pp. 11001–11006.

[61] A.A. Manenkov,"Ultimate laser intensities in transparent solids", *Laser Phys.*, 1996, **6**, 3, pp. 501-505.

[62] M.D. Perry, B.C. Stuart, P.S. Banks, M.D. Feit, V. Yanovsky, and A.M. Rubenchik, "Ultrashort-pulse laser machining of dielectric materials", *J. Appl. Phys.*, 1999, **85**, pp. 6803-6810.

[63] M.D. Perry, B.C. Stuart, P.S. Banks, M.D. Feit, and J.A. Sefcik, " Ultrashort-pulse laser micromachining", *LIA Handbook of Laser Materials Processing*, ed. J.F. Ready and D.F. Farson, Laser Institute of America, Magnolia Publishing, Inc., 2001, pp. 499-508.

[64] X. Mao, S.S. Mao, and R.E. Russo, "Imaging femtosecond laser-induced electronic excitation in glass", *Appl. Phys. Lett.*, 2003, **82**, pp. 697-699.

[65] M.V. Ammosov, N.B. Delone, and V.P. Krainov, "Tunnel ionization of complex atoms and of atomic ions in an alternating electromagnetic", *Soviet Phys. JETP*, 1986, **64**, pp. 1191-1194.

[66] D. Arnold and E. Cartier, "Theory of laser-induced free-electron heating and impact ionization in wide-band-gap solids", *Phys. Rev. B*, 1992, **46**, pp. 15102-15115.

[67] J. Jasapara, A.V.V. Nampoothiri, W. Rudolph, D. Ristau, and K. Starke, "Femtosecond laser pulse induced breakdown in dielectric thin films", *Phys. Rev. B*, 2001, **63**, pp. 045117-045121.

[68] X. Xu, G. Chen, and K.H. Song, "Experimental and numerical investigation of heat transfer and phase change phenomena during excimer laser interaction with nickel", *Int. J. Heat Mass Transfer*, 1999, **42**, pp. 1371-1382.

[69] M. Li, S. Menon, J.P. Nibarger, and G.N. Gibson, "Ultrafast Electron Dynamics in Femtosecond Optical Breakdown of Dielectrics", *Phys. Rev. Lett.*, 1999, **82**, pp. 2394-2397.

[70] N. Bloembergen, "Laser-induced electric breakdown in solids", *IEEE J. Quantum Electron*, 1974, **QE-10**, pp. 375-386.

[71] L.H. Holway and D.W. Fradin, "Electron avalanche breakdown by laser radiation in insulating crystals", *J. Appl. Phys.*, 1975, **46**, pp. 279- 291.

[72] M. Sparks, D.L. Mills, R. Warren, T. Holstein, A.A. Maradudin, L.J. Sham, E. Loh, Jr., and D.F.

King, "Theory of electron-avalanche breakdown in solids", *Phys. Rev. B*, 1981, **24**, pp. 3519-3536.

[73] A.A. Manenkov and A.M. Prokhorov "Laser-induced damage in solids," *Sov. Phys. Usp.* 1986, **148**, 1, pp. 179-211.

[74] D. Du, X. Liu, G. Korn, J. Squier, and G. Mourou, "Laser-induced breakdown by impact ionization in SiO_2 with pulse widths from 7 ns to 150 fs", *Appl. Phys. Lett*., 1994, **64**, pp. 3071-3074.

[75] D. Du, X. Liu, and G. Mourou, "Reduction of multi-photon ionization in dielectrics due to collisions", *Appl. Phys. B*, 1996, **63**, pp. 617-621.

[76] K. Yeom, H. Jiang, and J. Singh, "High power laser semiconductor interactions: a Monte Carlo study for silicon", *J. Appl. Phys.*, 1997, **81**, pp. 1807-1812.

[77] L. V. Keldysh, "Ionization in the field of a strong electromagnetic wave", *Sov. Phys. JETP*, 1965, **20**, pp. 1307-1314.

[78] M. D. Perry, A. Szoke, O. L. Landen, and E. M. Campbell, "Nonresonant multiphoton ionization of noble gases: Theory and experiment," *Phys. Rev. Lett.* 1988, **60**, pp. 1270-1273.

[79] G. Petite, S. Guizard, P. Martin, and F. Quéré, "Comment on 'Ultrafast electron dynamics in femtosecond optical breakdown of dielectrics'", *Phys. Rev. Lett*., 1999, **83**, pp. 5182.

[80] K.K. Thornber, "Applications of scaling to problems in high-field electronic transport", *J. Appl. Phys.*, 1981, **52**, pp. 279-290.

[81] Y.P. Raizer, *Laser-Induced Discharge Phenomena*, Consultant Bureau, New York, 1977.

[82] B. Luther-Davies, E.G. Gamaly, Y. Wang, A.V. Rode, and V.T. Tikhonchuk, "Matter in ultrastrong laser fields", *Sov. J. Quantum Electron*, 1992, **22**, pp. 289~325.

[83] M.V. Exter and A. Lagendijk, "Ultrashort surface-plasmon and phonon dynamics", *Phys. Rev. Lett*., 1988, **60**, pp. 49-52.

[84] S.S. Wellershoff, J. Hohlfeld, J. Gudde, and E. Matthias, "The role of electron-phonon coupling in femtosecond laser damage of metals", *Appl. Phys. A Suppl*., 1999, **69**, pp. 99-105.

[85] R. Gómez-Abal and W. Hübner**,** "Simple model for laser-induced electron dynamics", *Phys. Rev. B*, 2002, **65**, pp. 195114-195119.

[86] L.D. Landau and E.M. Lifshitz, *Electrodynamics of Continuous Media*, Pergamon, Oxford, 1960.

[87] E.M. Lifshitz and L.P. Pitaevskii, *Physical Kinetics*, Pergamon, Oxford, 1981.

[88] W. Rozmus and V.T. Tikhonchuk, "Skin effect and interaction of short laser pulses with dense plasmas", *Phys. Rev. A*, 1990, **42**, pp. 7401–7412.

[89] W.S. Fann, R. Storz, H.W.K. Tom, and J. Bokor, "Electron thermalization in gold", *Phys. Rev. B*, 1992, **46**, pp. 13592-13595.

[90] H. B. Sun, T. Tanaka, and S. Kawata, "Three-dimensional focal spots related to two-photon excitation", *Appl. Phys. Lett*., 2002, **80**, 20, pp. 3673-3675.

[91] L. Jiang and H.L. Tsai, "Unification of temperature concept in energy transport at microscale and macroscale", *Entropy*, 2003. (submitted)

[92] P. Stampfli and K.H. Bennemann, "Dynamical theory of the laser-induced lattice instability of silicon", *Phys. Rev. B*, 1992, **46**, 17, pp. 10686-10692.

[93] E.N. Glezer, Y. Siegal, L. Huang, and E. Mazur, "Behavior of ?(2) during a laser-induced phase transition in GaAs," *Phys. Rev. B*, 1995, **51**, 15, pp. 9589-9596.

[94] A. Miotello and R. Kelly, "Laser-induced phase explosion: new physical problems when a condensed phase approaches the thermodynamic critical temperature", *Appl. Phys. A Suppl*., 1999, **69**, pp. S67-S73.

[95] P.L. Silvestrelli, A. Alavi, M. Parrinello, and D. Frenkel, "Ab initio molecular dynamics simulation laser melting of silicon," *Phys. Rev. Lett*., 1996, **77**, 15, pp. 3149-3152.

[96] K. Sokolowski-Tinten, J. Bialkowski, M. Boing, and A. Cavalleri, D. von der Linde, "Thermal and nonthermal melting of gallium arsenide after femtosecond laser excitation", *Phys. Rev. B*, 1998b, **58**, pp. R11805-R11808.

[97] C. Cornaggia, in *Molecules and Clusters in Intense Laser Fields*, edited by J. Posthumus Cambridge University Press, Cambridge, U.K., 2001.

[98] M. Toulemonde, C. Dufour, A. Meftah, and E. Paumier, "Transient thermal processes in heavy ion irradiation of crystalline inorganic insulators", *Nucl. Instrum. Methods Phys. Res. B*, 2000, **166-167**, pp. 903-912.

[99] H.P. Cheng and J.D. Gillaspy, "Nanoscale modification of silicon surfaces via Coulomb explosion", *Phys. Rev. B*, 1997, **55**, pp. 2628-2636.

[100] R. Stoian, D. Ashkenasi, A. Rosenfeld, and E.E.B. Campbell, "Coulomb explosion in ultrashort pulsed laser ablation of Al_2O_3", *Phys. Rev. B*, 2000a, **62**, pp. 13167-13173.

[101] R. Stoian, H. Varel, A. Rosenfeld, D. Ashkenasi, R. Kelly, and E.E.B. Campbell, "Ion time-of-flight analysis of ultrashort pulsed laser-induced processing of Al_2O_3," *Appl. Surf. Sci*., 2000b, **165**, pp. 44-55.

[102] T. Brabec and F. Krausz, "Intense few-cycle laser fields: Frontiers of nonlinear optics," *Rev. of Mod. Phys.*, 2000, **72**, 2, pp. 545-591.

[103] V.P. Krainov and A.S. Roshchupkin, "Dynamics of the Coulomb explosion of large hydrogen iodide clusters irradiated by superintense ultrashort laser pulses," *Phys. Rev. A.*, 2001, **64**, pp. 063204~063208.

[104] A.C. Tam, H.K. Park, and C.P. Grigoropoulos, "Laser cleaning of surface contaminants", *Appl. Surf. Sci*., 1998, **127-129**, pp. 721-725.

[105] J.L. Brand and A.C. Tam, "Mechanism of picosecond ultraviolet laser sputtering of sapphire at 266 nm," *Appl. Phys. Lett*. 1990, **56**, pp. 883-885.

[106] D. Ashkenasi, A. Rosenfeld, H. Varel, M. Waehmer, and E. Campbell, "Laser processing of sapphire with picosecond and sub-picosecond pulses", *Appl. Surf. Sci*., 1997, **120**, pp. 65-80.

[107] R. Stoian, A. Rosenfeld, D. Ashkenasi, I.V. Hertel, N.M. Bulgakova, and E.E.B. Campbell, "Surface charging and impulsive ion ejection during ultrashort pulsed laser ablation", *Phys. Rev. Lett*., 2002, **88**, pp. 097603-097606.

[108] V. Schmidt, W. Husinsky, and G. Betz, "Dynamics of laser desorption and ablation of metals at the threshold on the femtosecond time scale", *Phys. Rev. Lett*., 2000, **85**, pp. 3516-3519.

[109] M. Ye and C.P. Grigoropoulos, "Time-of-flight and emission spectroscopy study of femtosecond laser ablation of titanium", *J. Appl. Phys.*, 2001, **89**, pp. 5183-5190

[110] V.Y. Bychenkov, V.T. Tikhonchuk, and S.V. Tolokonnikov, "Nuclear reactions triggered by laser-accelerated high-energy ions", *J. Exp. Theor. Phys.*, 1999, **88**, 6, pp. 1137-1142.

[111] H.O. Jeschke, M.E. Garcia, and K.H. Bennemann, **"**Theory for the ultrafast ablation of graphite films", *Phys. Rev. Lett*., 2001, **87**, pp. 015003-015006.

[112] J. Krüger and W. Kautek, "The femtosecond pulse laser: a new tool for micromaching", *Laser Phys.* 1999, **9**, pp. 30-40.